



**Universidade de São Paulo**

**Biblioteca Digital da Produção Intelectual - BDPI**

---

Departamento de Clínica Médica - FM/MCM

Artigos e Materiais de Revistas Científicas - FM/MCM

---

2012

# Post-receptor IGF1 insensitivity restricted to the MAPK pathway in a Silver-Russell syndrome patient with hypomethylation at the imprinting control region on chromosome 11

---

EUROPEAN JOURNAL OF ENDOCRINOLOGY, BRISTOL, v. 166, n. 3, pp. 543-550, MAR, 2012  
<http://www.producao.usp.br/handle/BDPI/42112>

*Downloaded from: Biblioteca Digital da Produção Intelectual - BDPI, Universidade de São Paulo*

## CASE REPORT

# Post-receptor IGF1 insensitivity restricted to the MAPK pathway in a Silver–Russell syndrome patient with hypomethylation at the imprinting control region on chromosome 11

Luciana R Montenegro<sup>1</sup>, Andrea C Leal<sup>1</sup>, Debora C Coutinho<sup>1</sup>, Helena P L Valassi<sup>1</sup>, Mirian Y Nishi<sup>1</sup>, Ivo J P Arnhold<sup>1</sup>, Berenice B Mendonca<sup>1</sup> and Alexander A L Jorge<sup>2</sup>

<sup>1</sup>Unidade de Endocrinologia do Desenvolvimento, Laboratorio de Hormonios e Genetica Molecular LIM/42 and <sup>2</sup>Unidade de Endocrinologia Genetica, Laboratorio de Endocrinologia Celular e Molecular LIM/25, Faculdade de Medicina da USP (LIM-25), Disciplina de Endocrinologia, Hospital das Clinicas da Faculdade de Medicina da Universidade de Sao Paulo, Avenida Dr Arnaldo, 455 5° andar sala 5340, CEP 01246-903 São Paulo – SP, Brazil

(Correspondence should be addressed to A A L Jorge; Email: alexj@usp.br)

## Abstract

**Background:** Hypomethylation of the paternal imprinting center region 1 (ICR1) is the most frequent molecular cause of Silver–Russell syndrome (SRS). Clinical evidence suggests that patients with this epimutation have mild IGF1 insensitivity.

**Objective:** To assess *in vitro* IGF1 action in fibroblast culture from a patient with SRS and IGF1 insensitivity.

**Methods:** Fibroblast cultures from one patient with SRS due to ICR1 demethylation and controls were established. The SRS patient has severe growth failure, elevated IGF1 level, and poor growth rate during human recombinant GH treatment. IGF1 action was assessed by cell proliferation, AKT, and p42/44-MAPK phosphorylation. Gene expression was determined by real-time PCR.

**Results:** Despite normal IGF1R sequence and expression, fibroblast proliferation induced by IGF1 was 50% lower in SRS fibroblasts in comparison with controls. IGF1 and insulin promoted a p42/44-MAPK activation in SRS fibroblasts 40 and 36%, respectively, lower than that in control fibroblasts. On the other hand, p42/44-MAPK activation induced by EGF stimulation was only slightly reduced (75% in SRS fibroblasts in comparison with control), suggesting a general impairment in MAPK pathway with a greater impairment of the stimulation induced by insulin and IGF1 than by EGF. A PCR array analysis disclosed a defect in MAPK pathway characterized by an increase in *DUSP4* and *MEF2C* gene expressions in patient fibroblasts.

**Conclusion:** A post-receptor IGF1 insensitivity was characterized in one patient with SRS and ICR1 hypomethylation. Although based on one unique severely affected patient, these results raise an intriguing mechanism to explain the postnatal growth impairment observed in SRS patients that needs confirmation in larger cohorts.

*European Journal of Endocrinology* 166 543–550

## Introduction

Silver–Russell syndrome (SRS, OMIM 180860) is a clinically and genetically heterogeneous disorder characterized by pre- and postnatal growth retardation, feeding difficulties in infancy, dysmorphic facial features (triangular shape face with normal head circumference, prominent forehead, small chin, and downturned corners of the mouth), fifth finger clinodactyly, and body asymmetry (1). The first molecular defect reported in patients with SRS was maternal uniparental disomy of chromosome 7 (mUPD7), identified in 5–11% of affected patients (1, 2, 3). The growth impairment caused by mUPD7 might be related to unidentified imprinted gene(s) located on this chromosome. In 2005, demethylation of the paternal imprinting center

region 1 (ICR1) located on chromosome 11 (11p15) was associated with SRS phenotype (4). The ICR1 is paternally methylated and controls the expression of insulin-like growth factor 2 (*IGF2*, OMIM 147470) and the noncoding *H19* gene. *IGF2* has a critical role in fetal growth and has a predominantly monoallelic expression from the methylated paternal allele during this period (4). Patients with SRS had a loss of methylation at ICR1, causing a reduction in *IGF2* expression. This epimutation was confirmed as the main molecular defect in SRS patients, being present in 43–64% of cases (2, 5).

Phenotypic characterization of children with SRS by hypomethylation at ICR1 revealed normal serum *IGF2* levels, probably reflecting hepatic production of *IGF2*, which is the main source of postnatal circulating *IGF2*

and biallelically expressed (5). Despite normal circulating IGF2 levels, these children failed to present catch-up growth in postnatal life. SRS children with hypomethylation at ICR1 have higher IGF1 levels than children with SRS caused by other molecular defects or non-SRS children born small for gestational age (SGA) (2). Normal or mildly elevated IGF1 levels with the absence of catch-up growth suggested that a mild form of insensitivity to IGF1 might explain the postnatal growth impairment observed in these children. Interestingly, higher levels of serum IGF-binding protein 3 (IGFBP3) were observed in these patients and could potentially be involved in the etiology of IGF insensitivity (2). Besides being the major carrier for circulating IGFs, IGFBP3 can act as a modulator of IGF bioactivity and has IGF1-independent actions on growth regulation at the tissue level (6). Animal models have indicated that overexpression of IGFBP3 is associated with intra-uterine and postnatal growth retardation despite elevated circulating IGF1 levels (7).

In this study, the IGF1 insensitivity observed in one SRS patient was characterized at clinical and molecular levels. The results strongly suggest that a post-receptor defect restricted to the MAPK pathway is responsible for IGF1 resistance observed in this SRS patient.

## Patients and methods

### Subject

The patient's parents provided written informed consent for clinical and genetic studies, and the study was approved by the ethics committee of the Hospital das Clinicas, University of Sao Paulo Medical School. The patient was born at 35 weeks of gestation by cesarean section following the diagnosis by prenatal ultrasound of intrauterine growth restriction. Length at birth was 35.5 cm ( $-5.2$  SDS for gestational age), birth weight was 1370 g ( $-3.0$  SDS), and the head circumference

was 32.5 cm ( $-1.5$  s.d.). Relative macrocephaly, cleft palate, clinodactyly, and penoscrotal transposition were present. The patient had body asymmetry and dysmorphic facial features compatible with SRS, scoring 13 out of 15 points on the SRS severity score (score  $\geq 8$  is diagnostic for SRS) (8). He is the first child from nonconsanguineous parents of Japanese descent. The father's height is 163 cm and the mother's height is 150 cm (target height SDS of  $-1.3$ ). His younger brother had normal pre- and postnatal growth (height SDS = 0.1).

At first evaluation at 6.9 years of age, he was 92.5 cm tall ( $-5.4$  s.d.), weighed 10.1 kg (BMI SDS =  $-4.8$ ), his head circumference was 49 cm ( $-1.8$  s.d.), and presented normal psychomotor development. Results of routine laboratory assessments were normal, as were thyroid function and karyotype. He had an adequate nutritional status, good socioeconomic condition, absence of signs of malnutrition, and normal total blood count, ferritin, and albumin. IGF1 and IGFBP3 levels were in the upper normal range (Table 1), whereas IGF2 (372 ng/ml) was in normal range. GH peak in response to oral clonidine stimulation test was 32 ng/ml at 60 min, which is considered an exaggerated response in our unit (9).

Human recombinant GH (rhGH) therapy was initiated (66  $\mu\text{g}/\text{kg}$  per day), and only a mild improvement in his growth rate was observed during therapy, despite elevated IGF1 and IGFBP3 levels (Table 1). At the beginning of the third year of therapy, the patient entered puberty at the age of 10 years with a height of 112 cm ( $-4.2$  s.d.) and a bone age of 10 years. Depot GNRH agonist (GNRHa) was added to suppress puberty (3.75 mg depot leuprolide acetate subcutaneously every 28 days). After 4 years of treatment, depot GNRHa therapy was discontinued and he presented normal pubertal development. At the last clinical visit, he was 16.9 years old, his height velocity was 1.2 cm/year, his height was 147 cm ( $-4.0$  SDS), and the rhGH

**Table 1** Growth velocity, IGF1 and IGFBP3 levels during human recombinant GH (rhGH) therapy (66  $\mu\text{g}/\text{kg}$  per day) in the Silver–Russell syndrome patient.

	Age (years)	rhGH dose ( $\mu\text{g}/\text{kg}$ per day)	Growth velocity (cm/year)	IGF1		IGFBP3		Glucose (mM)	Insulin (mU/l)
				$\mu\text{g}/\text{l}$	SDS	mg/l	SDS		
Basal	6.9	–	–	324	1.9	4.9	1.2		
Basal	7.0	–	5.2	450	2.1	4.0	0.5	5.1	7.0
First year of rhGH therapy	8.1	66	6.9	810	4.0	5.6	2.9	4.7	15.0
Second year	9.2	66	6.6	1000	5.6	6.1	2.7	4.6	3.0
Third year <sup>a</sup>	10.0	66	5.3	990	7.9	7.1	2.0	4.5	19.0
Fourth year <sup>b</sup>	11.0	100	7.3	1200	7.8	7.2	1.7	4.9	20.0
Fifth year <sup>b</sup>	12.0	90	6.5	1200	5.7	6.7	1.1	4.4	7.0
Seventh year	13.9	83	5.8	846	2.3	6.2	0.5	NA	NA
At the end of rhGH therapy <sup>c</sup>	16.9	80	1.1	1303	4.0	6.8	0.7	4.9	27.0

NA, not available.

<sup>a</sup>Patient entered puberty (LH 1.6 U/l and testosterone 1.66 nmol).

<sup>b</sup>Depot GNRH agonist (GNRHa) was associated to rhGH.

<sup>c</sup>GNRHa therapy was suspended.

treatment was stopped. Glucose and insulin levels were normal during the follow-up (Table 1). Due to the pre- and postnatal severe growth impairment and the poor growth response to rhGH despite high IGF1 levels (Fig. 1), IGF1 insensitivity was established clinically.

### Molecular studies

The coding region and intron boundary regions of *IGF1* (10) and IGF receptor type 1 (*IGF1R*) genes was amplified (primer sequences and amplification protocols available on request) and PCR products were directly sequenced by the dideoxy chain-termination method using a dye terminator kit and analyzed in an ABI Prism 3100 automated sequencer (Applied Biosystems, Foster City, CA, USA). Maternal uniparental disomy was investigated by genotyping four microsatellite markers located on 7p12–15. The imprinting center region 1 (ICR1) contains seven CTCF target sites in the differentially methylated regions (DMR) 2 kb upstream of H19. Methylation of the H19DMR in 11p15 was analyzed by a commercially available methylation-sensitive multiplex ligation probe-dependent amplification

(MLPA) test (assay MEO30BWS/RSS; MRC Holland, Amsterdam, The Netherlands) (11). Reactions and analysis were performed according to the manufacturer's instructions (Microsoft Cops.).

### Cell cultures

Fibroblast cultures were established from skin biopsies taken from the forearm of the hypotrophic side of the patient with SRS at the age of 12 years and from three control individuals: one 30-year-old adult (C2) with normal pre- and postnatal growth and two age- and sex-matched children: one 12-year-old boy with normal birth weight and length (C1), and a 15-year-old boy born SGA with normal *IGF1R* gene and ICR1 methylation profile. Cell cultures were maintained in DMEM (Invitrogen Life Technologies, Inc.) supplemented with 20% fetal bovine serum (12), 50 IU/ml penicillin, and 50 mg/ml streptomycin at 37 °C in 5% CO<sub>2</sub>. All studies were performed between passages 3 and 10).

### Proliferation assay

The effect of IGF1 on fibroblast proliferation was analyzed using the commercially available 3-(4,5-dimethylthiazol-2-yl)-5-(3-carboxymethoxyphenyl)-2-(4-sulfophenyl)-2H-tetrazolium (MTS) assay according to the manufacturer's recommendations (CellTiter 96 Aqueous One Solution; Promega) (13). Briefly, cells were seeded into 96-well plates (5000 cells/well). Three wells were used for each treatment condition: serum-free medium (SFM) (negative control), 5% FCS (positive control), and increasing IGF1 concentrations (10, 25, and 50 ng/ml). Twenty microliters of MTS inner salt and phenazine ethosulfate were added to each well. MTS was reduced into a colored formazan product by the living cells. The amount of formazan product was measured at a wavelength of 490 nm and is directly proportional to the number of cells in each well. Experiments were performed in triplicate and results were confirmed by two independent experiments.

### Immunoblotting

Confluent fibroblasts were incubated with SFM overnight and subsequently treated with SFM, IGF1, or desIGF1 ([Arg3]-IGF1-des(1–3)IGF1) for 20 min. Afterward, cells were washed with ice-cold PBS (10 mM sodium phosphate, pH 7.4, 150 mM NaCl) and resuspended in lysis buffer (100 mM Tris, pH 7.5, containing 10 mM EDTA, 10 mM sodium fluoride, 100 mM sodium pyrophosphate, 1% Nonidet P-40 (octyl phenoxypolyethoxyethanol), 1% sodium deoxycholate, 2 mM Na<sub>3</sub>VO<sub>4</sub>, 10 mM NaF, 1 mM phenylmethylsulphonyl fluoride, 1 µg/ml leupeptin, 1 µg/ml aprotinin, and 1 µg/ml pepstatin). Samples were

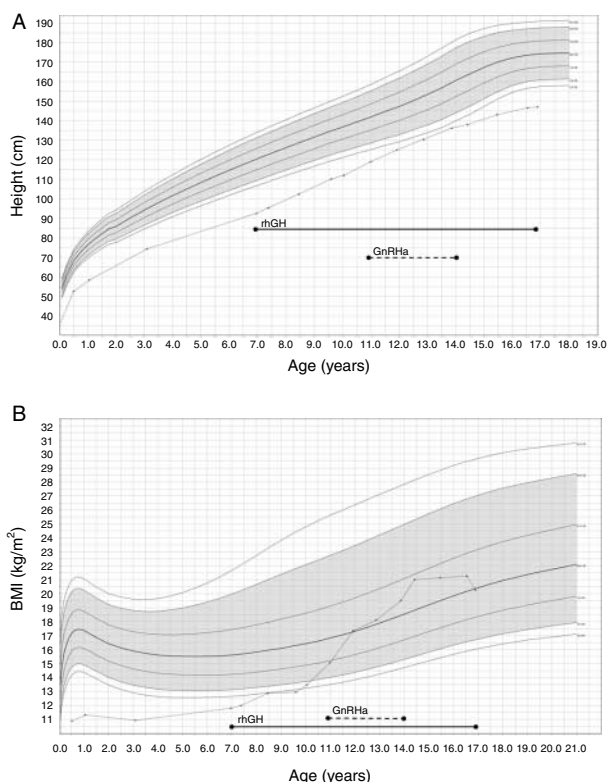


**Figure 1** Height (A) and BMI (B) for age charts of SRS patient. Growth charts were drawn using Growth Analyser 3.5 (Ed. Dutch Growth Foundation, PO Box 23068, 3001 KB, Rotterdam, The Netherlands). rhGH treatment is shown as solid line, whereas GNRHa treatment is shown as a dashed line.

resolved by SDS-PAGE, transferred onto nitrocellulose membranes, and probed with specific antibodies. Bound antibodies were detected using the enhanced chemiluminescence (ECL) system and read in an optical scanner (Storm; Molecular Dynamics, Inc., Sunnyvale, CA, USA). Blots were subsequently stripped (10 mM Tris-HCl, pH 7.5, 0.5 M  $\beta$ -mercaptoethanol, 8 M urea, 1.5 M BSA at 65 °C for 20 min) and reincubated with a distinct antibody for normalization. Each experiment was performed in triplicate.

IGFBP3 secretion was also evaluated. Confluent fibroblast cultures grown on 6-well plates were washed with PBS and incubated for 36 h with a SFM. Conditioned medium was collected and total protein concentration determined by the micro LOWRY Kit (Sigma-Aldrich) for normalization. Equivalent volumes of culture media, containing similar amounts of total protein, were concentrated using Ultracel YM-30 filters (Millipore, Billerica, MA, USA). Samples were resolved by SDS-PAGE, transferred onto nitrocellulose membranes, and probed with a specific IGFBP3 antibody. Each experiment was performed in triplicate.

### Real-time PCR

Total RNA was extracted from confluent fibroblast cell cultures and peripheral leukocytes using TRIzol reagent (Invitrogen Life Technologies, Inc.) (14). The extracted RNA was reverse transcribed using the High-Capacity cDNA Archive Kit (Applied Biosystems). Subsequently, cDNA was analyzed by quantitative real-time PCR in an ABI Prism 7700 sequence detector using TaqMan gene expression assays for quantification (*IGF1R*, Hs00181385\_m1 and *IGFBP3*, Hs00181211\_m1; Applied Biosystems) according to the manufacturer's instructions. Furthermore, Human MAP Kinase Signaling Pathway PCR Array (ID assay 4414076; Applied Biosystems) was performed to assess the expression of 92 genes related to the MAPK signaling pathway (Supplementary Table 1, see section on supplementary data given at the end of this article). All target genes with cycle number of threshold value ( $C_t$ ) > 35 were considered not detectable and were excluded from the analysis. Four endogenous control genes were used for each sample, and the reactions were performed in triplicate. Relative expression levels were calculated using the  $2^{-\Delta\Delta C_t}$  method (15). Mean expression of target gene in C1 fibroblast lineage was assigned expression values of 1.0, and fold increase in expression levels was determined for each cell culture sample. All results were confirmed using at least two independent assays.

### Materials

Human recombinant IGF1 (hIGF1) and recombinant [Arg3]-IGF1-des(1-3)IGF1 (desIGF1) were purchased from Upstate Biotechnology, Inc. (Lake Placid, NY, USA). Recombinant human EGF was purchased from

BioSource (Camarillo, CA, USA). CellTiter 96 proliferation assay kit (Promega) was used in proliferation assays. Micro Lowry kit (Sigma-Aldrich) was used for determination of protein concentration and Ultracel YM-30 (Millipore) for protein concentration. The ECL detection system and antimouse and antirabbit IgG conjugated to HRP were obtained from Amersham Pharmacia Biotech. Prestained molecular weight standards were purchased from Invitrogen (Invitrogen Life Technologies, Inc.). The following primary antibodies were used: anti-IGFBP3 from Upstate Biotechnology (cat. 06-108); anti-IGF1R  $\beta$ -subunit (cat. sc-713), anti-phospho-AKT1/2 (Ser 473; cat. sc-7985), and anti-AKT1/2 (cat. sc-8312) from Santa Cruz Biotechnology, Inc. (Santa Cruz, CA, USA); and anti-phospho-MAPK (Tyr202/Thr204; cat. 36-8800) and anti-MAPK (cat. 13-6200) from Invitrogen Life Technologies, Inc.

### Statistical analysis

Quantitative variables are shown as mean  $\pm$  S.E.M. and were analyzed by unpaired Student's *t*-test or one-way ANOVA and Tukey *post hoc* tests. A *P* value < 0.05 was considered significant. All statistical analyses were performed using SigmaStat version 3.5 (Systat Software, Inc., Chicago, IL, USA).

## Results

### Molecular genetics

mUPD7 was ruled out by microsatellite analysis. Hypomethylation of the H19DMR (ICR1) with normal methylation profile at the IGF2DMR was observed in genomic DNA from peripheral leukocytes, as well as from fibroblasts (passages 7-9) of the patient with SRS. No mutation was detected in *IGF1* and *IGF1R* genes.

### In vitro characterization of IGF1 insensitivity

Fibroblasts from the patient with SRS had a significantly reduced proliferative response to IGF1 in comparison with the age-matched control ( $55 \pm 5\%$  of C1 proliferative response, Fig. 2A) as well as in comparison with other controls ( $48 \pm 2\%$  of C2 and  $56 \pm 14\%$  of SGA proliferative response). These results support the presence of IGF1 insensitivity in the SRS patient, in agreement with clinical and laboratory findings. Expression of *IGF1R* mRNA in SRS fibroblasts was 1.9-fold higher than in C1 fibroblasts but did not reach statistical significance ( $P=0.07$ ; Fig. 2B). However, the total content of IGF1R was similar in controls and SRS fibroblasts (Fig. 2C). These results indicate that the IGF1 insensitivity observed in fibroblasts from the SRS patient is not caused by quantitative alterations in IGF1R.

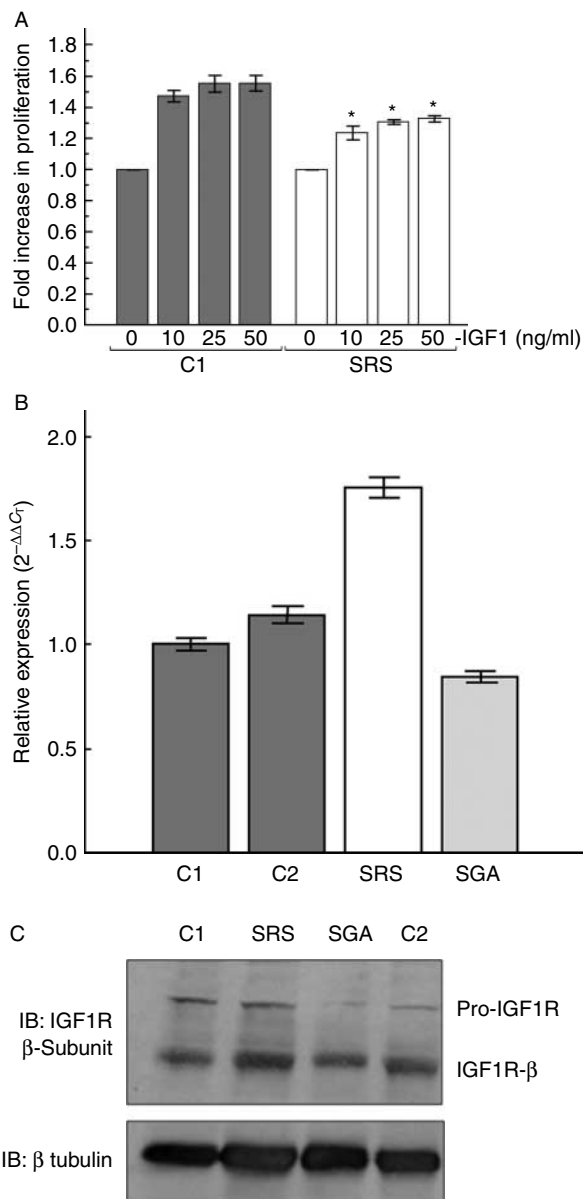


**Figure 2** (A) Cell proliferation response to different IGF1 doses for 36 h. Results are shown as fold increase in proliferation rate in relation to untreated fibroblasts and expressed as mean  $\pm$  1 s.e.m. of three independent experiments. \*Significant difference between SRS fibroblasts and fibroblasts from age-matched control (C1) ( $P < 0.05$ ). (B) Analysis of *IGF1R* mRNA expression in fibroblasts from the SRS patient (SRS), non-SRS SGA patient (SGA), and controls (C1 and C2). Results are expressed in relation to *IGF1R* expression in C1 fibroblasts (mean  $\pm$  1 s.e.m. of three independent experiments). (C) IGF1R protein evaluation in control 1, SRS, SGA, and control 2 fibroblasts. Blots shown are representative of three independent experiments with equivalent results.

### Impaired p42/44-MAPK phosphorylation but normal AKT phosphorylation after IGF1 stimulation in fibroblasts from the patient with SRS

Fibroblasts from SRS and non-SRS SGA patients exhibited normal activation of the phosphoinositide 3-kinase (PI3K) pathway, assessed by AKT phosphorylation, in comparison with controls (Fig. 3A). Despite similar total contents of p42/44-MAPK, SRS fibroblasts had lower basal and post-IGF1 stimulation p42/44-MAPK phosphorylation levels, 52 and 40%, respectively, when compared with C1 ( $P < 0.001$ ; Fig. 3B). Treatment with increasing doses of IGF1 did not normalize p42/44-MAPK phosphorylation in SRS fibroblasts (Fig. 3B). Insulin treatment promoted a p42/44-MAPK activation in SRS fibroblasts which was 36% lower than in control fibroblasts; on the other hand, p42/44-MAPK activation induced by EGF stimulation was only slightly reduced (75% in SRS fibroblasts in comparison with controls, Fig. 3C).

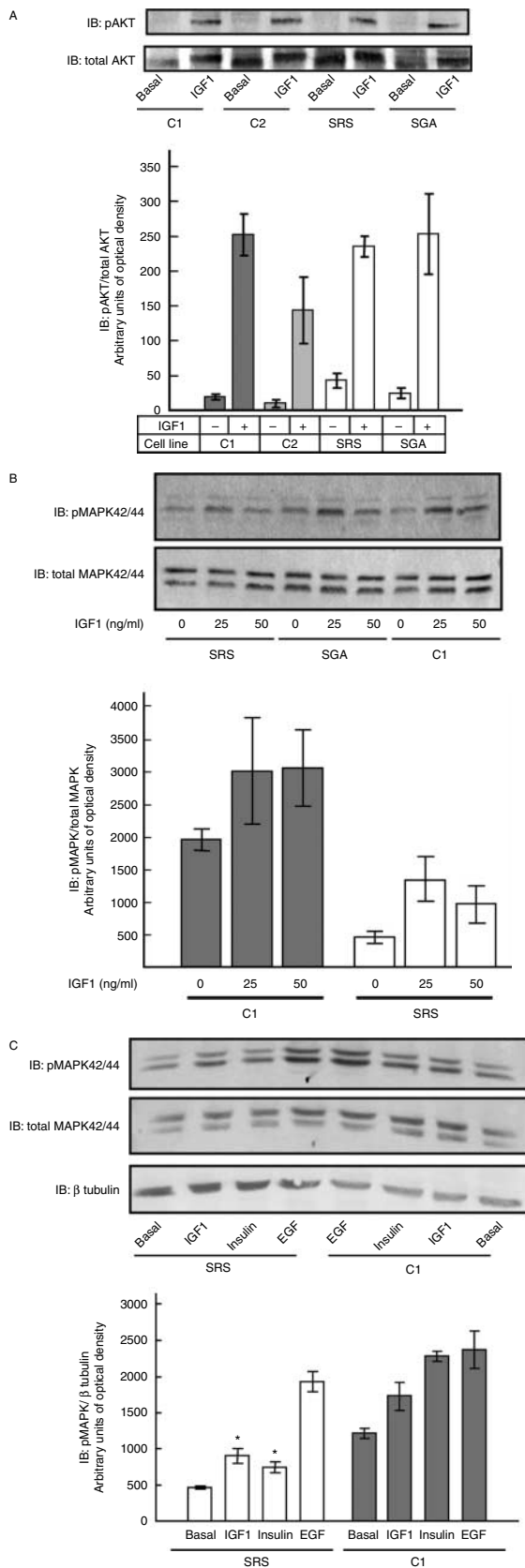
### Increased IGFBP3 expression in fibroblasts from the patient with SRS results in increased IGFBP3 secretion

Previous clinical data suggested that increased IGFBP3 levels in patients with SRS could be involved in IGF1 insensitivity (2), and therefore, the expression of *IGFBP3* mRNA in fibroblasts of our patient with SRS was analyzed by real-time PCR. Expression of *IGFBP3* was significantly increased (14-fold increase,  $P < 0.001$ ) in SRS fibroblasts in comparison with controls (Fig. 4A). Moreover, IGFBP3 expression in culture medium was twofold increased in the SRS culture in comparison with controls ( $P < 0.001$ ), demonstrating increased IGFBP3 secretion by SRS fibroblasts (Fig. 4B).

To investigate the role of elevated IGFBP3 on IGF1 insensitivity in SRS fibroblasts, cell proliferation and p42/44-MAPK activation were assessed after stimulation with desIGF1, an IGF1 analog with low affinity for IGFBPs that retains the ability to activate IGF1R (16). In control fibroblasts, stimulation with desIGF1 induced similar degrees of proliferation and p42/44-MAPK phosphorylation to those induced by IGF1 (Fig. 4C). However, in SRS fibroblasts, there was no improvement in proliferation rate or MAPK pathway activation with desIGF1. This result suggests that IGF1 insensitivity in SRS cells is not directly mediated by IGF1 binding to IGFBP3.

### Analysis of the expression of MAPK pathway-related genes in patient fibroblast

To identify abnormal expression in genes related to the MAPK signaling, a PCR array analyzing 92 genes of this pathway was performed. Expression of dual specificity phosphatase 4 (*DUSP4*) and myocyte



enhancer factor 2C (*MEF2C*) was significantly increased (threefold) in fibroblasts from the patient with SRS in comparison with controls ( $P < 0.001$ , Supplementary Table 1).

## Discussion

Hypomethylation of ICR1 at 11p15 is the most frequent molecular cause of SRS. There is evidence that patients with this epimutation present mild IGF1 insensitivity characterized by the absence of catch-up growth and normal or moderately high IGF1 and IGF2 levels in postnatal life (2). IGFs exert most of their growth effects through IGF1R, a tyrosine kinase receptor essential for pre- and postnatal normal growth (17). In this study, we investigated IGF1 action in a fibroblast culture from a patient with SRS and severe IGF1 insensitivity. This patient presented hypomethylation of ICR1, elevated IGF1 levels, and poor growth response to rhGH therapy. IGF1 failed to induce normal proliferation of this patient's fibroblasts *in vitro* indicating IGF1 insensitivity at the cellular level. No mutations in *IGF1* or *IGF1R* were observed. In addition, SRS fibroblasts expressed *IGF1R* normally at mRNA and protein levels; nevertheless, this cell line had impairment of MAPK activation despite normal AKT activation, suggesting a post-receptor defect compromising only the MAPK pathway. Similar results were obtained when patient fibroblasts were stimulated with insulin and EGF, suggesting a general impairment in MAPK pathway in SRS patient's fibroblasts.

Further molecular studies showed that expression of *IGFBP3* was increased in SRS fibroblasts. These results are in agreement with previous reports of clinical findings in SRS patients with epimutations of ICR1 who presented high IGFBP3 serum levels (2). IGFBP3 can act as a modulator of IGF1 bioactivity and has IGF1-independent actions on growth regulation at the tissue level. SRS fibroblasts were treated with desIGF1, an IGF1 analog with low affinity for IGFBPs (16). desIGF1 was unable to restore proliferation rates and MAPK activation in fibroblasts from the patient with SRS. These results suggest that impairment of IGF1 binding to its receptor due to IGFBP3 increase does not explain the observed MAPK pathway defect.

**Figure 3** Evaluation of the PI3K (A) and MAPK (B and C) pathway activation by IGF1. Serum-starved fibroblasts were incubated with or without IGF1 (25 ng/ml), insulin (100 nM), or EGF (50 ng/ml) for 20 min, as indicated. Cell lysates were resolved by SDS-PAGE, transferred onto nitrocellulose, and probed with a specific antibody recognizing phospho-p42/44-MAPK (Tyr202/Thr204) or phospho-AKT1/2 (Ser 473). The blot was stripped and reprobed with a specific antibody recognizing total p42/44-MAPK, total AKT1/2, or  $\beta$ -tubulin as indicated. Blots shown are representative of at least three independent experiments with equivalent results. Bands were quantified by densitometry and normalized by total protein. Vertical bars represent mean  $\pm$  S.E.M. of three independent experiments ( $*P < 0.001$ ).

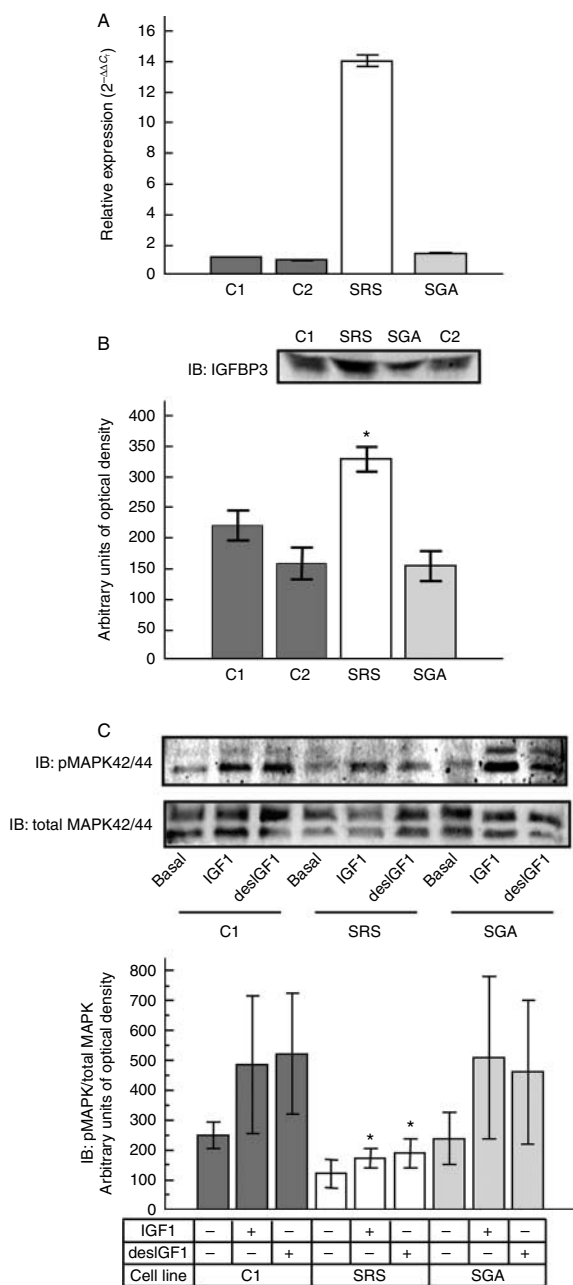


**Figure 4** (A) Expression of *IGFBP3* mRNA in SRS, non-SRS SGA, and control fibroblasts. Results are expressed in relation to *IGFBP3* expression levels in C1 fibroblasts. (B) *IGFBP3* secretion into cell culture media by confluent SRS and control fibroblasts. Vertical bars represent mean  $\pm$  S.E.M. of three independent experiments (\* $P < 0.001$ ). (C) Evaluation of the MAPK pathways activation by IGF1 or desIGF1 (25 ng/ml) for 20 min, as indicated. Blots shown are representative of at least three independent experiments with equivalent results. Bands were quantified by densitometry and normalized by total protein. Vertical bars represent mean  $\pm$  S.E.M. of three independent experiments. \*A significant difference in expression levels was observed between SRS fibroblasts and controls ( $P < 0.001$ ).

The RAS–MAPK pathway involves several intracellular proteins that communicate a signal from a receptor on the surface of the cell to the DNA in the nucleus, controlling fundamental cellular processes such as growth, proliferation, differentiation, migration, and apoptosis. p42/44-MAPK phosphorylation reflects the adequate capacity of cell membrane receptors to activate this kinase cascade. In an attempt to identify the defect in RAS–MAPK signaling observed in our patient’s fibroblasts, a real-time PCR array analyzing 92 genes in this pathway was performed. An increase in *DUSP4* and *MEF2C* expression was observed in the SRS patient fibroblasts. *MEF2C* has a role in myogenesis. The encoded protein, MEF2 polypeptide C, is activated by IGF1 and participates in IGF1-induced cardiac hypertrophy through p38-MAPK phosphorylation (1). However, the exact role of *MEF2C* on global IGF1 signaling is unknown (18). *DUSP4* encodes a member of the dual specificity protein phosphatase subfamily, which dephosphorylates both phosphothreonine and phosphotyrosine residues in MAPKs, inactivates MAPK signaling, and thereby inhibits cellular proliferation (19). *DUSP4* was recently implicated as a novel tumor suppressor gene and its expression can be modulated by differential methylation in the promoter region (20). Patients with SRS and hypomethylation of *ICR1* can also have methylation anomalies at other loci (21). Unfortunately, we were unable to demonstrate difference in the methylation profile at *DUSP4* promoter region in our patient (data not shown). Further studies are necessary to investigate the possibility of other methylation abnormalities to explain the increase in *DUSP4* expression.

In summary, a post-IGF1R signaling abnormality associated with IGF1 insensitivity was characterized in one severely affected patient with SRS and *ICR1* hypomethylation. Our results suggest a defect in the MAPK pathway in this patient, involving an increase in *DUSP4* expression, a molecule implicated in the inactivation of MAPK signaling. Although our study was based on one unique severely affected patient, the present results raise an intriguing possibility to explain the postnatal growth impairment observed in patients with SRS. Analyses of larger cohorts are needed to explore the role of specific MAPK pathway defects mediating growth failure in patients with SRS.

**Supplementary data**

This is linked to the online version of the paper at <http://dx.doi.org/10.1530/EJE-11-0964>.

**Declaration of interest**

The authors declare that there is no conflict of interest that could be perceived as prejudicing the impartiality of the research reported.



## Funding

This work was supported by grants from Fundacao de Amparo a Pesquisa do Estado de Sao Paulo (FAPESP) (08/57915-2 to A C Leal, 05/04726-0 and 05/50144-2 to L R Montenegro) and from Conselho Nacional de Desenvolvimento Cientifico e Tecnologico (CNPq) (142062/06-5 to D C Coutinho; 301339/2008-9 to B B Mendonca; 300938/06-3 to I J P Arnhold and 307951/06-5 to A A L Jorge). The authors are indebted to Bruno F Souza for language review.

## References

- 1 Abu-Amero S, Monk D, Frost J, Preece M, Stanier P & Moore GE. The genetic aetiology of Silver–Russell syndrome. *Journal of Medical Genetics* 2008 **45** 193–199. (doi:10.1136/jmg.2007.053017)
- 2 Binder G, Seidel AK, Martin DD, Schweizer R, Schwarze CP, Wollmann HA, Eggermann T & Ranke MB. The endocrine phenotype in Silver–Russell syndrome is defined by the underlying epigenetic alteration. *Journal of Clinical Endocrinology and Metabolism* 2008 **93** 1402–1407. (doi:10.1210/jc.2007-1897)
- 3 Kotzot D. Maternal uniparental disomy 7 and Silver–Russell syndrome – clinical update and comparison with other subgroups. *European Journal of Medical Genetics* 2008 **51** 444–451. (doi:10.1016/j.ejmg.2008.06.001)
- 4 Gicquel C, Rossignol S, Cabrol S, Houang M, Steunou V, Barbu V, Danton F, Thibaud N, Le Merrer M, Burglen L, Bertrand AM, Netchine I & Le Bouc Y. Epimutation of the telomeric imprinting center region on chromosome 11p15 in Silver–Russell syndrome. *Nature Genetics* 2005 **37** 1003–1007. (doi:10.1038/ng1629)
- 5 Netchine I, Rossignol S, Dufourg MN, Azzi S, Rousseau A, Perin L, Houang M, Steunou V, Esteve B, Thibaud N, Demay MC, Danton F, Petriczko E, Bertrand AM, Heinrichs C, Carel JC, Loeuille GA, Pinto G, Jacquemont ML, Gicquel C, Cabrol S & Le Bouc Y. 11p15 imprinting center region 1 loss of methylation is a common and specific cause of typical Silver–Russell syndrome: clinical scoring system and epigenetic–phenotypic correlations. *Journal of Clinical Endocrinology and Metabolism* 2007 **92** 3148–3154. (doi:10.1210/jc.2007-0354)
- 6 Firth SM & Baxter RC. Cellular actions of the insulin-like growth factor binding proteins. *Endocrine Reviews* 2002 **23** 824–854. (doi:10.1210/er.2001-0033)
- 7 Modric T, Silha JV, Shi Z, Gui Y, Suwanichkul A, Durham SK, Powell DR & Murphy LJ. Silver–Russell syndrome: clinical scoring system and epigenetic–phenotypic correlations. *Journal of Clinical Endocrinology and Metabolism* 2001 **142** 1958–1967. (doi:10.1210/en.142.5.1958)
- 8 Bartholdi D, Krajewska-Walasek M, Ounap K, Gaspar H, Chrzanowska KH, Ilyana H, Kayserili H, Lurie IW, Schinzel A & Baumer A. Epigenetic mutations of the imprinted IGF2-H19 domain in Silver–Russell syndrome (SRS): results from a large cohort of patients with SRS and SRS-like phenotypes. *Journal of Medical Genetics* 2009 **46** 192–197. (doi:10.1136/jmg.2008.061820)
- 9 Silva EG, Shlessarenko N, Arnhold IJ, Batista MC, Estefan V, Osorio MG, Marui S & Mendonca BB. GH values after clonidine stimulation measured by immunofluorometric assay in normal prepubertal children and GH-deficient patients. *Hormone Research* 2003 **59** 229–233. (doi:10.1159/000070222)
- 10 Coutinho DC, Coletta RR, Costa EM, Pachi PR, Boguszewski MC, Damiani D, Mendonca BB, Arnhold IJ & Jorge AA. Polymorphisms identified in the upstream core polyadenylation signal of IGF1 gene exon 6 do not cause pre- and postnatal growth impairment. *Journal of Clinical Endocrinology and Metabolism* 2007 **92** 4889–4892. (doi:10.1210/jc.2007-1661)
- 11 Eggermann T, Schonherr N, Eggermann K, Buiting K, Ranke MB, Wollmann HA & Binder G. Use of multiplex ligation-dependent probe amplification increases the detection rate for 11p15 epigenetic alterations in Silver–Russell syndrome. *Clinical Genetics* 2008 **73** 79–84. (doi:10.1111/j.1399-0004.2007.00930.x)
- 12 Coelho JC & Giugliani R. Fibroblasts of skin fragments as a tool for the investigation of genetic diseases: technical recommendations. *Genetics and Molecular Biology* 2000 **23** 269–271. (doi:10.1590/S1415-47572000000200004)
- 13 Tada H, Shiho O, Kuroshima K, Koyama M & Tsukamoto K. An improved colorimetric assay for interleukin 2. *Journal of Immunological Methods* 1986 **93** 157–165. (doi:10.1016/0022-1759(86)90183-3)
- 14 Chomczynski P & Sacchi N. Single-step method of RNA isolation by acid guanidinium thiocyanate–phenol–chloroform extraction. *Analytical Biochemistry* 1987 **162** 156–159. (doi:10.1016/0003-2697(87)90021-2)
- 15 Livak KJ & Schmittgen TD. Analysis of relative gene expression data using real-time quantitative PCR and the 2<sup>−</sup>(Delta Delta C(T)) method. *Methods* 2001 **25** 402–408. (doi:10.1006/meth.2001.1262)
- 16 Francis GL, Ross M, Ballard FJ, Milner SJ, Senn C, McNeil KA, Wallace JC, King R & Wells JR. Novel recombinant fusion protein analogues of insulin-like growth factor (IGF)-I indicate the relative importance of IGF-binding protein and receptor binding for enhanced biological potency. *Journal of Molecular Endocrinology* 1992 **8** 213–223. (doi:10.1677/jme.0.0080213)
- 17 Abuzzahab MJ, Schneider A, Goddard A, Grigorescu F, Lautier C, Keller E, Kiess W, Klammt J, Kratzsch J, Osgood D, Pfaffle R, Raile K, Seidel B, Smith RJ & Chernausek SD. IGF-I receptor mutations resulting in intrauterine and postnatal growth retardation. *New England Journal of Medicine* 2003 **349** 2211–2222. (doi:10.1056/NEJMoa010107)
- 18 Munoz JP, Collao A, Chiong M, Maldonado C, Adasme T, Carrasco L, Ocaranza P, Bravo R, Gonzalez L, Diaz-Araya G, Hidalgo C & Lavandero S. The transcription factor MEF2C mediates cardiomyocyte hypertrophy induced by IGF-1 signaling. *Biochemical and Biophysical Research Communications* 2009 **388** 155–160. (doi:10.1016/j.bbrc.2009.07.147)
- 19 Patterson KI, Brummer T, O'Brien PM & Daly RJ. Dual-specificity phosphatases: critical regulators with diverse cellular targets. *Biochemical Journal* 2009 **418** 475–489. (doi:10.1042/BJ20082234)
- 20 Waha A, Felsberg J, Hartmann W, von dem Knesebeck A, Mikeska T, Joos S, Wolter M, Koch A, Yan PS, Endl E, Wiestler OD, Reifenberger G & Pietsch T. Epigenetic down-regulation of mitogen-activated protein kinase phosphatase MKP-2 relieves its growth suppressive activity in glioma cells. *Cancer Research* 2010 **70** 1689–1699. (doi:10.1158/0008-5472.CAN-09-3218)
- 21 Turner CL, Mackay DM, Callaway JL, Docherty LE, Poole RL, Bullman H, Lever M, Castle BM, Kivuva EC, Turnpenny PD, Mehta SG, Mansour S, Wakeling EL, Mathew V, Madden J, Davies JH & Temple IK. Methylation analysis of 79 patients with growth restriction reveals novel patterns of methylation change at imprinted loci. *European Journal of Human Genetics* 2010 **18** 648–655. (doi:10.1038/ejhg.2009.246)

Received 11 July 2011

Revised version received 5 December 2011

Accepted 13 December 2011